Optical modulation in photonic band gap structures by surface acoustic waves

Srinivasan Krishnamurthy[a] and Paulo V. Santos
Paul-Drude-Institut and für Festkörperelektronik, Hausvogteiplatz 5-7, 10117 Berlin, Germany

(Received 5 December 2003; accepted 11 May 2004)

We investigate theoretically the modulation of light beams in photonic band gap (PBG) structures by surface acoustic waves (SAWs). In these structures, the propagation of light beams can be actively controlled through an external acoustic stimulus. We have extended the mathematically rigorous transfer matrix method to calculate the light flow in PBG structures subjected to the spatial- and time-dependent dielectric function modulation induced by the SAW. The calculational procedure, which applies for SAWs with a frequency much smaller than that of the light, is employed to determine the transmission spectra of a one-dimensional Bragg stack with a cavity and that of a two-dimensional GaAs PBG structure with periodic air holes. We demonstrate that these two structures can be configured as an on/off optical switch with very high contrast ratios and, in the two-dimensional case as an efficient wavelength-tunable optical filter. © *2004 American Institute of Physics*. [DOI: 10.1063/1.1767974]

I. INTRODUCTION

The expected device size limits in semiconductor technology, the explosion of telecommunication and network traffic, and the need for optical computation lead to intensified search for efficient optical systems. There has been considerable effort to develop components for optical network and optical computational applications such as switches and dense wavelength division multiplexers (DWDMs).[1] Frequency tunability, high contrast ratio between the transmitting (or "on") state and the reflecting (or "off") states, ease of fabrication, and integration have been the main goals of this research effort. In this respect, materials with nonlinear or piezoelectric properties are ideally suited for optical modulation applications.

Photonic band gap (PBG) materials offer an additional degree of freedom to tailor the light propagation properties by controlling the dimensions of basic dielectric units to submicrometer sizes.[2] Until now, PBG structures have mainly been used as passive optical elements, such as Bragg mirrors, light cavities, and waveguides. Recently, there have been many efforts to turn them into active devices by modulating the dimensions or the dielectric function of the medium.[3–8] The modulation has been achieved by dynamically changing the temperature,[4,5] electric field (through the optical Stark effect),[4,8] material density,[2,3] and carrier density.[9,10]

In this paper, we study PBG-based switching devices, which rely on the dielectric modulation induced by a surface acoustic wave (SAW).[3,7,11,12] Although not explicitly stated, most of the concepts and results also apply to bulk acoustic modes. The use of SAWs in the place of bulk acoustic waves has a few advantages.[13,14] SAWs with frequencies in the gigahertz range and high power densities can be efficiently generated electrically using inter-digital transducers (IDTs) on piezoelectric materials such as GaAs.[7,15,16] The fabrication of the IDTs employs conventional semiconductor technologies and on-chip integration of SAW devices becomes possible. We note, however, that there have been considerable progresses in the generation and optical modulation by bulk acoustic wave in semiconductor structures with frequencies in the tetrahertz range.[17]

In an unstructured material, a SAW creates a periodic modulation of the optical properties with the SAW wavelength λ_{SAW} and frequency ω_s. The latter is normally much smaller than that of the light. In a perturbative approach, the periodic variation provides the necessary scattering wave vector ($\mathbf{k}_{SAW}$) for coupling light modes in the linear light dispersion as illustrated in Fig. 1. In a normal scattering process (labeled as *A* in Fig. 1), a light mode with wave vector $\mathbf{k}_0$ is coupled with another one of wave vector $-\mathbf{k}_0$ by a collinear SAW with a wave vector $\mathbf{k}_{SAW}$. This interaction results in the Bragg reflection of the light beam. Note that the energy of the SAW is much smaller than that of light and only *horizontal* (i.e., with negligible change in light energy) scattering processes are allowed. The energy and momentum conservation thus restrict the light modes (denoted by $\mathbf{k}_0$)

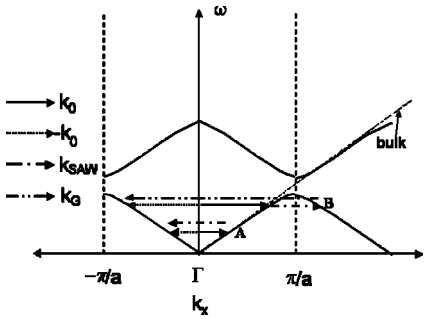

FIG. 1. Light dispersion in an unstructured (dashed line) and in an one-dimensional PBG structure. The arrows indicate a direct (a) and an umklapp (b) scattering process induced by a SAW with wave vector $\mathbf{k}_{SAW}$, which can be employed for frequency-tunable light filter.

[a]Author to whom correspondence should be addressed; permanent address: SRI International, Menlo Park, CA 94025; electronic mail: srini@aristotle.sri.com

that can be scattered by a SAW (with wave vector $\mathbf{k}_{SAW}$). The other light modes remain undisturbed.[3,7,11,12]

For light beams in the near infrared region, the Bragg reflection for collinear SAW and light propagation requires very small SAW wavelengths (equal to half of the optical wavelength in the material) and, thus, very high SAW frequencies. The requirements can be relaxed in a PBG material, where a static structural modulation induces a periodic change in the refractive index with a periodicity a comparable to the light wavelength. This periodicity folds the dispersion of light modes into a mini-Brillouin zone extending from $-\pi/a$ it to in π/a, as illustrated for a simple one-dimensional (1D) PBG structure in Fig. 1. When a SAW with $\lambda_{SAW} \gg a$ is applied to the PBG structure, an additional modulation is imposed on the dielectric function. This periodic variation provides the necessary $\mathbf{k}_{SAW}$ for coupling light modes in the folded photonic dispersion through an umklapp process involving a grating wave vector $\mathbf{k}_G$ with magnitude $2\pi/a$, also illustrated at B in Fig. 1, where $\mathbf{k}_0+\mathbf{k}_{SAW}+\mathbf{k}_G=-\mathbf{k}_0$.[7,11] If the light and the SAW beam are not collinear, the scattered vector $-\mathbf{k}_0$ corresponds to a ray propagating along a different angle as the incident one.

The procedure can be applied to select a particular light wavelength by controlling ω_s (and, thus, $\mathbf{k}_{SAW}$), an important feature for wavelength tunable filters. By using a bulk acoustic wave to provide the required coarse peniodicity in a 3 mm-long Bragg fiber, Liu and co-workers[3] have demonstrated a tunable light reflection filter where the light wavelength is determined by the SAW wavelength. The operation of the tunable filter is based on the umklapp process as described in the preceding paragraph. Due to the weak acousto-optic (AO) interaction, many periods of the acoustic modulation were required to get a noticeable contrast between the transmitting and reflecting states. Previous studies have addressed the modulation of tunable filters based on layered structures by acoustic modes.[7,11] In this paper, we investigate a similar filter based on the modulation of a two-dimensional (2D) PBS structure.

For applications such as light switching, a high contrast between the "on" and the "off" states becomes an important issue. One way to achieve high contrast switching with a short interaction paths between the light and the SAW beams explores the use of photonic cavities.[18] When Bragg mirrors with high-contrast dielectric materials are used, the band gap in the light energy dispersion is large, while the "defect" states introduced in the gap by the cavity layer have a narrow energy distribution. Because of the strong localization of the electromagnetic field, the AO interaction becomes significantly enhanced in the cavity region, thus resulting in a high dielectric modulation. The strong modulation is obtained at the cost of a reduced frequency tunability.

On the theoretical side, there are three well established techniques to calculate light propagation in PBG structures: the plane wave,[2] the transfer matrix (TM),[19–21] and the finite-difference time-domain methods.[22] While the plane-wave method, which is performed in the frequency domain, is easy to implement, its computational time increases as the cube of the system size. Noting that Maxwell's equations are local, the band structure calculations can progress in order "N"

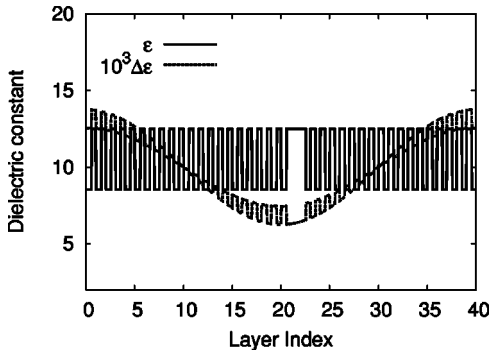

FIG. 2. Dielectric constant (solid line) and dielectric modulation by an acoustic wave (dashed line) in a one-dimension PBG structure consisting of a GaAs cavity inserted in-between asymmetric GaAs/AlAs Bragg mirrors.

scaling by switching to the time domain. However, since our main interest resides in the calculation of transmission and reflection spectra, we found it more appropriate to use the efficient TM method. From the calculational point of view, the long-range periodic dielectric modulation induced by the SAW increases the basic unit cell size of the PBG structures by one to two orders of magnitude. In addition, the SAW modulation is time dependent, leading to transmission and reflection through channels shifted in frequency by a multiple of the SAW frequency.

In this paper, we extend the TM method to study light modulation in PBG structures induced by SAW. The required changes to the original TM method as well as a brief outline to calculate SAW-induced dielectric variation in PBG structures are discussed in Secs. II and III, respectively. The method is applied in Sec. IV A to a 1D asymmetric Bragg mirror with a cavity and to a 2D structure in Sec. IV B. The conclusions are summarized in Sec. V. A summary of results for 1D structures has been communicated for publication elsewhere.[18] The details of the calculation procedure and its extension to 2D structures are given here.

II. THE TM METHOD

In PBG crystals, a structural modulation is used to create a periodic change in the refractive index (and, consequently, in the dielectric function) with a periodicity comparable to the light wavelength.[2] In the TM method,[19–21] Maxwell's equations are recast so that the fields in one period of the structure are connected to those in the next one. This process is repeated until the reflected and transmitted intensities are related to the incident intensity. When a SAW with a wavelength λ_s much longer than the periodicity of the underlying PBG structure propagates across the structure, an additional time-dependent periodicity is superimposed on its dielectric function, as shown in Fig. 2. The solution of Maxwell's equations has to include the effects of both the short- and the long-range periodicities. We have extended the mathematically rigorous TM method to the case, where the unit cell in the direction of light propagation is a multiple of λ_s and the dielectric function varies with the SAW frequency ω_s. Two main changes have been introduced in the conventional TM method. First, the size of the basic unit was increased to include all PBG unit cells within one wavelength of the

SAW. Second, since under the time-dependent modulation the transmission and reflection take place through channels of frequencies $(\omega_0 \pm m\omega_s)$, with $m=0,1,2,\ldots$,[7] the TM method has to take into account modes of different frequency as well as the coupling between them. This effect has been included by increasing the dimensions of the propagation matrices by a factor $(2m+1)$ as compared to the conventional TM method. In the present calculations, we neglected modes with $m \geqslant 2$, so that size of the transmission and reflection matrices becomes three times as large as that for a bare PBG structure (i.e., in the absence of a SAW). Care has been taken to avoid the numerical instability arising on account of the increase in the number of forward steps *and* in the matrix dimensions. Except for these modifications, which will be described in more details below, our method is simply an extension of the original TM method of Pendry *et al.*,[19,20] so that several mathematical steps already treated will be skipped here. All notations have the same meaning as in TM method treatment.[19,20]

We start with the two Maxwell's equations describing light propagation in the absence of free charges and currents,

$$\nabla \times \mathbf{E} = = -\frac{\partial \mathbf{B}}{\partial t}$$

$$\nabla \times \mathbf{E} = = -\frac{\partial \mathbf{D}}{\partial t} \tag{2.1}$$

where the electric (**E**), displacement (**D**), magnetic induction (**B**), and magnetic (**H**) fields of incident plane wave are described as

$$\mathbf{D} = \epsilon_0 \epsilon(\omega_s)\mathbf{E},$$

$$\mathbf{E} = \mathbf{E}_0 e^{i(\mathbf{k}\cdot\mathbf{r}-\omega_0 t)},$$

$$\mathbf{B} = \mathbf{B}_0 e^{i(\mathbf{k}\cdot\mathbf{r}-\omega_0 t)},$$

$$\mathbf{H} = \mu_0 \mu \mathbf{B} \tag{2.2}$$

with

$$\epsilon(\omega_s) = \overline{\epsilon}(\mathbf{r}) + \frac{\Delta\epsilon(\mathbf{r})}{2}(e^{i\omega_s t} + e^{-i\omega_s t}). \tag{2.3}$$

$\overline{\epsilon}(\mathbf{r})$ represents the spatially dependent dielectric function of the PBG structure in the absence of a SAW and $\Delta\epsilon(\mathbf{r})$ the modulation introduced by the SAW. This modulation is determined by $\mathbf{k}_{\mathrm{SAW}}$. Although the Eq. (2.2) indicates the use of a standing SAW, this calculational procedure can be easily modified for the case of a propagating SAW. We note, however, that the use of a standing wave is advantageous, since it leads for a higher modulation efficiency for the same acoustic power.[23] Substituting Eq. (2.2) into Eq. (2.1) and noting that ω_sw is much smaller than ω_0, we get

$$\mathbf{k} \times \mathbf{E} = \omega_0 \mathbf{B},$$

$$\mathbf{k} \times \mathbf{H} = -\omega_0 \epsilon_0 \epsilon(\omega_s)\mathbf{E}. \tag{2.4}$$

The last form is identical to the original formulation in Ref. 19, except that the dielectric function is now given by Eq. (2.3). Once cast in this form, the original TM expressions[19] to connect the fields of one layer to the next are still valid. Since $\Delta\epsilon$ is very small (≈ 0.01) when compared to $\overline{\epsilon}(\approx 10)$, we performed the following approximation:

$$\frac{1}{\epsilon(\omega_s)} = \frac{1}{\overline{\epsilon}}\left[1 - \frac{\Delta\epsilon}{2\overline{\epsilon}}(e^{i\omega_s t} + e^{-i\omega_s t})\right]. \tag{2.5}$$

In the linear approximation leading to Eq. (2.5), the TM expressions for fields clearly separate into terms arising from the channels at frequencies $\omega_0 - \omega_s$, ω_0, and $\omega_0 + \omega_s$. Each field component A_i (**A** can be **E** or **H**) can be written as a sum of three terms;

$$A_i = \overline{A_i} + \Delta\mathbf{A_i}(e^{i\omega_s t} + e^{-i\omega_s t}).$$

If we change the basis set ψ_r, from (**E**,**H**) (Refs. 19 and 20) to

$$\psi_r = \begin{pmatrix} E_x(r)e^{-i\omega_s t} \\ E_y(r)e^{-i\omega_s t} \\ H_x(r)e^{-i\omega_s t} \\ H_y(r)e^{-i\omega_s t} \\ E_x(r) \\ E_y(r) \\ H_x(r) \\ H_y(r) \\ E_x(r)e^{i\omega_s t} \\ E_y(r)e^{i\omega_s t} \\ H_x(r)e^{i\omega_s t} \\ H_y(r)e^{i\omega_s t} \end{pmatrix}, \tag{2.6}$$

then the transfer matrix T relates the fields at the position $\mathbf{r}+\mathbf{c}$ to that at the position **r** by, $T\psi_r = \psi_{r+c}$ as in the conventional TM formalism. However, the T matrix takes the form,

$$T = \begin{bmatrix} T_0 & \Delta T & 0 \\ \Delta T & T_0 & \Delta T \\ 0 & \Delta T & T_0 \end{bmatrix}. \tag{2.7}$$

Here, T_0 is the T matrix of the unperturbed system (i.e., without a SAW), while ΔT represents the correction arising from the time-dependent modulation of the dielectric function by the SAW. Each of these submatrices is of size 4×4 for each (x,y) mesh point in the unit cell.

In order to obtain the transmission and reflection coefficients, the basis set of Eq. (2.6) has to be projected onto forward and backward propagating plane waves. The T matrix of Eq. (2.7) has to be recast in the plane-wave basis. If So is the required matrix to transform the basis to the plane-wave basis in the unperturbed case, then

$$S = \begin{bmatrix} S_0 & 0 & 0 \\ 0 & S_0 & 0 \\ 0 & 0 & S_0 \end{bmatrix}$$

will transform our new basis of Eq. (2.6) to the plane-wave basis. Each submatrix component of Eq. (2.7) can be transformed as in the unperturbed case. Then, a straightforward

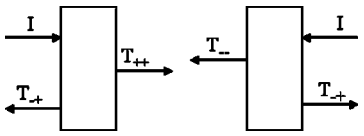

FIG. 3. Definitions of transmission and reflection coefficients.

rearrangement of the matrix elements will lead to a projected T matrix in the familiar form,

$$T = \begin{bmatrix} T^{++} & T^{+-} \\ T^{-+} & T^{--} \end{bmatrix}, \tag{2.8}$$

where each of the submatrices is of the size 6×6 for each (x,y) mesh point of the unit cell (i.e., three times larger than those in the unperturbed system). Correspondingly, the size of transmission and reflection matrices is also increased by a factor of 3. They are now given by

$$t^{\pm\pm} = \begin{bmatrix} t_0^{\pm\pm} & t_-^{\pm\pm} & 0 \\ t_-^{\pm\pm} & t_0^{\pm\pm} & t_+^{\pm\pm} \\ 0 & t_+^{\pm\pm} & t_0^{\pm\pm} \end{bmatrix}. \tag{2.9}$$

where the subscripts 0 and ± represent the central (ω_0) and frequency-shifted $(\omega_0 \pm \omega_s)$ channels of transmission and reflection. In the unperturbed case, where the incident plane wave impinges from the left, there will be one transmission (T^{++}) and one reflection matrix (T^{-+}), as shown in Fig. 3. However, in the presence of a SAW, there will be three transmission and three reflection coefficients (one for each channel i). The corresponding transmissions and reflections are denoted as $|t_i^{++}|^2$ and $|t_i^{-+}|^2$, respectively. A similar definition applies for an incident wave coming from the right. A pictorial definition of these quantities is given in Fig. 3. Except for increased size, all quantities keep their unperturbed form. Hence, as in the case of the unperturbed system, these transmission and reflection quantities $(t_i^{\pm\pm})$ are easily obtained in terms of the submatrices of Eq. (2.8).

A straightforward implementation of transfer matrix formalism to thicker PBGs often lead to numerical instability, owing to the exponentially growing solutions. Since the form of the transfer matrices is preserved in the modified expressions [Eqs. (2.6)–(2.9), the various clever tricks, particularly the multiple scattering approach, used in the original formalism to circumvent numerical instabilities and also to accelerate the computation can also be used here. We still keep the step length in the wave propagation direction the same as that in the other directions. However, the PBG unit cell is divided into a number of subcells, and the fields are directly evaluated only in those subcells. Then, the multiple scattering formalism is repeatedly used to transport the transmission matrices from one end of the structure to the other end. We found that the calculations are numerically stable even when the supercell contains 300 PBG cells.

III. ACOUSTIC INTERACTION

The expressions derived in the preceding section can be used to calculate the wavelength dependence of the light transmission and reflection coefficients for a given device structure modulated by a SAW. The model requires as input the amplitude of the dielectric modulation $\Delta\epsilon$ induced by the SAW. The procedure to obtain $\Delta\epsilon$ has been described elsewhere.[7]

In order to apply the formalism to a real situation, two additional approximations become necessary. The first is related to the fact that the SAW reduces the symmetry of the cubic crystal so that $\Delta\epsilon$ becomes a tensor. This 3×3 dielectric tensor is obtained in terms of the photoelastic coefficients and the amplitudes of the strain field generated by the SAW at 1 μm below the surface. The implicit assumption of constant strain at this depth is reasonable when the waveguide width is much smaller than the SAW wavelength, which is assumed to be 5.6 μm in the present calculations. If the off-diagonal components of the tensor are small, we can determine the refractive index modulation can be obtained from the component of $\Delta\epsilon$ along the particular light polarization. We restrict ourselves to this approximation.

The second approximation is associated with the changes in the dimensions of the photonic structures by the SAW strain field, which introduces a mechanical contribution to the dielectric modulation. This effect can be easily taken into account in the case of 1D layered structures by including the changes in thickness of the individual layers induced by the strain.[24] For a 2D structure, however, a similar procedure requires a fine discretization grid, which considerably increases the computation times and were not included in the present calculations. We use an effective dielectric modulation,[25] which simultaneously takes into account both the mechanical and the conventional elasto-optic contributions.

IV. RESULTS AND DISCUSSION

A. 1D Bragg cavity

As a test of the accuracy of the calculation procedure, we first applied it to a Bragg fiber structure similar to the one investigated by Liu *et al.*[3] The Bragg fiber corresponds closely to a 1DPBG structure with dispersion similar to the one shown in Fig. 1. The structural parameters of the fiber were assumed to be the same as in Ref. 3: a Bragg periodicity of 508 nm, an average refractive index of 1.5, an acoustic wavelength of 102 μm, and a peak value of $\eta = \Delta\epsilon/\epsilon = 6\times 10^{-3}$ for the modulation of the dielectric constant by the SAW. For these parameters, we calculated a central wavelength of $\lambda_0 = 1526.5$ nm and a stop-band width of 0.7 nm (from 1526.2 to 1526.9 nm). Under a SAW, additional reflections with intensity corresponding to 10% of that of the incident radiation were found at 1526 and 1527.1 nm. These reflection lines correspond to the umklapp scattering processes indicated in Fig. 1.[3] We note that the light modes involved in the scattering are near the edges, where the low group velocity of the light leads to an enhanced AO interaction with the SAW (cf. Fig. 1). In spite of that and of the long device length, the reflection coefficients are quite small (of about only 0.1) in this 1D structure, in agreement with the experimental observations.[3] Further increase in acoustic power, device length, and in the dielectric contrast in the Bragg grating are needed to improve the reflectivity.

Longer SAW wavelengths restrict the scattering to light modes very close to the edges of the stop band, further reducing the light group velocity and increasing the AO interaction. However, in order to maintain the wave vector conservation required for wavelength selectivity, the device length has also to be increased to accommodate several SAW periods. In the case of semiconductor-based structures, a further constraint is dictated by the deposition of high quality 1D stacks of layers with a high dielectric contrast. For sophisticated procedures such as molecular-beam epitaxy or chemical-vapor-deposition methods, the maximum stack thickness is limited to a few micrometers.

It is our interest to find shorter structures that offer large AO modulation for lower acoustic intensities. Since the AO interaction can be increased at the localized defect states in the gap of a PBG structure, where the light field is strongly concentrated, we recently proposed an optical modulator or switch that employs a 1D Bragg stack with a cavity.[18] Alternatively, one can employ 2D PBG structure similar to the one studied in the literature,[26,27] which we will consider in Sec. IV B.

In the following, we apply the calculation procedure of Sec. II to a design, which combines an optical cavity within 1D asymmetric Bragg mirror and the AO effect to modulate an incident light beam. When Bragg mirrors with high-contrast dielectric materials are used, the stop band widens, while the width of the "defect" or cavity states created in the stop band narrows. The photon motion is restricted to a very small energy range: this effect has been successfully used for several applications. Recently, an optical modulator with a contrast ratio of 5 based on the optical Stark effect in a GaAs cavity had been demonstrated.[8] The strong localization of electric field in the cavity has been shown to increase the acoustooptic interaction.[28] The field concentration together with the large changes in the refractive index predicted for energies close to the band gap[16] of GaAs are expected to lead to very high-contrast modulation.

Due to the lack of periodicity in the direction perpendicular to the cavity layer (x direction), the wave vector $\mathbf{k}_x$ is no longer a good quantum number to describe the cavity states. The scattering takes place when the energy conservation condition is satisfied. For ease of fabrication, we consider thin and planar structures, which can be grown with the current molecular-beam-epitaxy (MBE) technology. The composition and thickness of the layers as well as the total size of the layer stack were varied so as to enhance the interaction between light of wavelength of 940 nm and a SAW with $\lambda_s = 5.6\ \mu$m. The electric field concentration in the cavity is crucial for the enhancement of the AO interaction. We found that the modulation is the largest when the cavity with optical thickness $\lambda/2$ is placed close to, but not exactly at the center of the Bragg mirror structure composed of $\lambda/4$ dielectric layers. One possible structure is shown in Fig. 2. It is a 40-period asymmetric Bragg structure with a GaAs cavity near the center. The first 21 periods are alternating AlAs and GaAs layers with thicknesses of 76.9 and 65.5 nm, respectively, followed by the 142.4 nm-thick GaAs cavity and the second mirror, which has 18 periods with the same composition as the first Bragg mirror. This structure exhibits a forbidden gap of 117 nm (from 865 to 983 nm), as shown in the transmission spectrum of Fig. 4. The cavity states are located near 940 nm and have a full width at half maximum (FWHM) of about 0.5 nm. Although this design is for operation near 940 nm, the structure can be easily scaled for other operation frequencies.

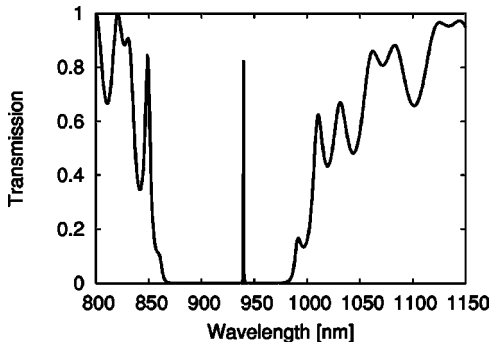

FIG. 4. Calculated transmission coefficient for the structure given in Fig. 1 in the absence of a SAW. The sharp line at 940 nm corresponds to the cavity resonance.

In our calculations, we assumed that the SAW creates a sinusoidal modulation of the dielectric constant as shown in Fig. 2. The change in the dielectric constant η was calculated from the SAW strain field. For that purpose, the strain distribution for a SAW with frequency ω_s and linear power density θ propagating in a $(\mathrm{AI},\mathrm{Ga})\mathrm{As}$ layered structure were obtained using an elastic model.[7] The strain field induced by the SAW varies with the depth from the surface. We used in the calculation a maximum value of $\eta = 6\times10^{-4}$, which corresponds to dielectric modulation for TE light at a depth of 1 μm from the surface, induced by a 500 MHz Rayleigh SAW on GaAs (100) with a linear power density of 20 W/m. The transmission coefficient t_0 of the cavity calculated over a wide wavelength region is displayed in Fig. 4. The stop band covers the range from 865 to 983 nm. The cavity mode appears as a sharp line, which is shown in detail by the open circles in Fig. 5. Under a SAW, an incident light beam with central frequency ω_0 induces reflection and transmission through frequency-shifted channels $\omega_0+\omega_s$ and $\omega_0-\omega_s$. In Fig. 5, the calculated transmission coefficients through the central channel $[t(\omega_0),\mathrm{dots}]$ and side channels $[t(\omega_0\pm\omega_s),\mathrm{squares}]$ are compared with the one obtained in the absence of a SAW [t_0, open circles]. Note that there is

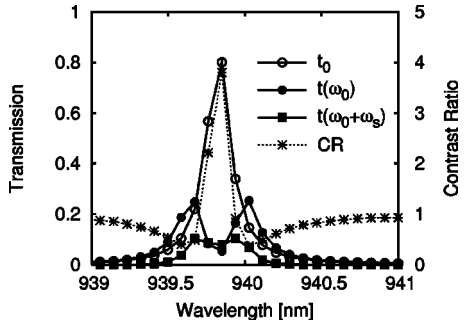

FIG. 5. Calculated transmission coefficient near $\omega_0 = 940$ nm for the structure given in Fig. 2 with (solid symbols) and without a SAW (open symbols). The wavelength scale is in the vicinity of the cavity resonance displayed in Fig. 4. The dotted line shows the contrast ratio CR.

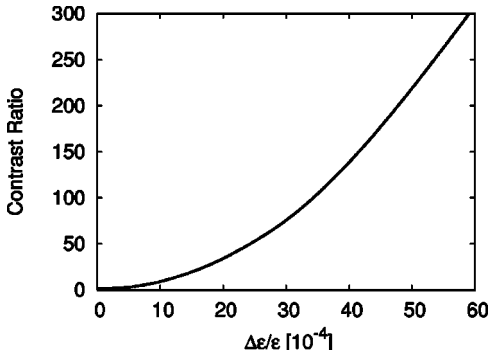

FIG. 6. Expected contrast ratio of the 1D optical switch as a function the dielectric modulation $\eta=\Delta\epsilon/\epsilon$

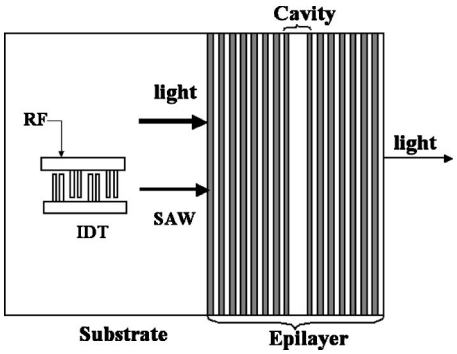

FIG. 7. One-dimensional cavity structure modulated by a SAW.

considerable scattering both *within* and between the channels. The inter- and the intra-channel scattering modes have negligible intensities except for frequencies very close to the cavity states, where the AO interaction is enhanced. Although the transmission occurs through all three frequencies, the channels are separated by the very small SAW frequency $\omega_s \ll \omega_0$. In continuous-wave (cw) experiments, the observed transmission coefficient will thus be the sum of the contributions from all three channels. Hence, the contrast ratio(CR) is defined as the ratio of t_0 to $[t(\omega_0)+t(\omega_0+\omega_s)+t(\omega_0-\omega_s)]$ and plotted as a dashed line in Fig. 5. A maximum CR of about 4 can be obtained even for a weak SAW intensity.

We find that it is possible to increase η to values of up to $\eta=4\times10^{-3}$ for a 500 MHz SAW in GaAs by an appropriate design of the IDTs.[24,25] Previous calculations for a specific design[13] within the GaAs/(Al,Ga) As system show that much larger η's (of up to 2.3×10^{-2}) are possible. To investigate the operation of the switch under these conditions, we show in Fig. 6 the calculated CRs for various values of η. CR increases almost quadratically with η, reaching values as high as 300 for $\eta=0.6\%$ (corresponding to a relative refractive index change of 0.3%). One can expect, in this case, a nearly perfect on/off switching action if η reaches the predicted[16] maximum of 2.3×10^{-2}.

Layer thickness fluctuations inherent to the growth techniques will affect the CR. This effect was modeled by assuming that the dielectric constants fluctuates randomly within 5% of their original values. We found that the highest CR decreases from 300 to 240, while the central frequency may shift due to changes in the cavity thickness.

Although the structure proposed here can be grown by the MBE method, an unconventional placement of the IDT for SAW generation may be required. Since the dimensions of IDT for high frequency SAWs (>1 GHz) can be significantly reduced below 1 mm, we suggest its placement on the *side* of the substrate, as shown in Fig. 7. In this configuration, both the SAW and the light beams travel along the direction perpendicular to the layer stack. Recent developments of electron-beam lithography and of imprint techniques[29] for IDT fabrication may make such an arrangement possible. Another possibility is to generate the SAW on a highly piezoelectric material, such as $LiNbO_3$ or ZnO, and then to couple it to the device structure on GaAs employing wafer bonding techniques.

B. 2D planar device

The major advantages of the 1D optical switch proposed in the preceding section are potentially very high contrast ratios, short switching times (≈1 μs), extremely small size, and externally controlled modulation. However, the dynamic frequency tunability (i.e., the selection of ω_0) in the cavity-based optical switch is limited, if any, to the nanometer-wide range defined by the defect states. If more defect states are introduced to increase the resonance width and, thus, the tunability range, the AO interaction will be reduced because of the delocalization of the electric field and, thus, the photon residence time in the cavity region. The devices have to be made longer, since the probability for AO interaction increases with the residence time. The maximum thicknesses of the 1D Bragg stack, however, is restricted by the film deposition techniques to a few micrometer.

In this subsection, we show that the tunability properties can be considerably improved by using a SAW to modulate a short, 2D PBG structure. A similar concept has been applied previously to 1-D structures.[7,11] Both because of increased dielectric contrast and the increased parameter space offered by the 2D nature of the PBG structure, the modulation performance is optimized. We further show that the rejection frequency can be dynamically tuned within a large bandwidth with a minimal change in the SAW wavelength, a feature of particular relevance for DWDM applications.

We consider the 2D structure consisting of an array of deep air holes on GaAs epilayers displayed in Fig. 8. Such structures have been proposed and fabricated in the past for photonic applications.[26,27] We have studied the effect of a SAW on the transmission characteristics of a 44 μm-long 2D structure, in which air holes of radius of 103 nm are arranged in a square lattice with a periodicity of 275 nm. The 2D planar structure is amenable for the placement on the path of

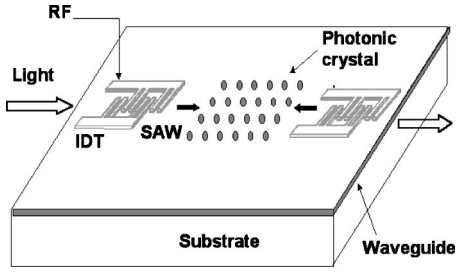

FIG. 8. Proposed two-dimensional PBG structure based on semiconductors.

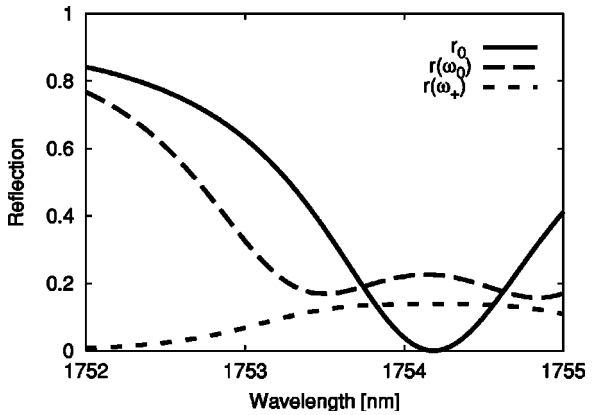

FIG. 9. Calculated reflection coefficient near the resonance wavelength of 1754 nm for the structure given in Fig. 8 in the absence of a SAW (solid line) and under a SAW with wavelength of 5.5 μm for the unshifted [$r(\omega_0)$, dashed line] and for the up-shifted [$r(\omega_0+\omega_s)$, dotted line] modes.

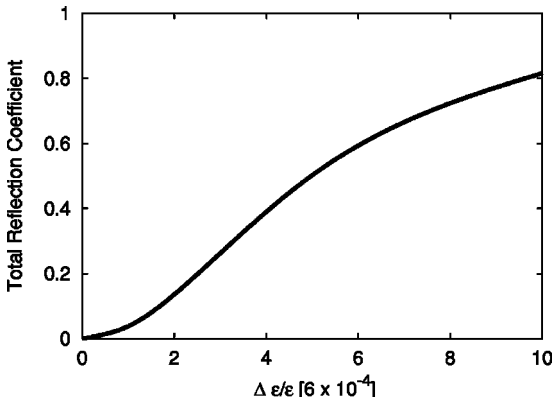

FIG. 10. Expected total reflection coefficient of the 2D structure of Fig. 8 as a function of $\eta=\Delta\epsilon/\epsilon$.

a SAW generated by an IDT. The light impinges from a waveguide placed a fraction of λ_{SAW} below the surface and propagates in the same direction as the SAW. For the present design, the TM mode exhibits the lowest forbidden gap for photon wavelengths between 1360 and 1740 nm.

The transmission and reflection for light wavelengths above 1740 nm is characterized by Fabry-Perot oscillations arising from the interference of the incoming light beam with the reflected at the output interface of the PBG region. The spectral positions of the reflection minima depend on the total thickness of the structured region. In our Bragg structure, this thickness was chosen to yield a reflection minimum at the resonance frequency ω_0 (corresponding to a wavelength of 1754.2 nm) in the absence of a SAW, as indicated by the solid line denoted as r_0 in Fig. 9.

In the presence of a SAW with $\lambda_{SAW}=5.5$ μm, the momentum (or wave vector) conservation for the umklapp process (indicated by B in Fig. 1) is satisfied for an incident light with frequency ω_0. Hence, modifications in the transmission and reflection are expected near the ω_0, $\omega_0+\omega_s$ and $\omega_0-\omega_s$, channels. The calculated reflection coefficient in the vicinity of these frequencies for $\eta=3\times10^{-3}$ is displayed in Fig. 9. The dotted and dashed lines show the reflection coefficients $r(\omega_0)$ and $r(\omega_0+\omega_s)$ through the center and the up-shifted channels, respectively. Since we use a standing SAW in our calculations, the reflection through the $\omega_0+\omega_s$ and $\omega_0-\omega_s$ channels are always equal. The reflection through these channels increases from zero in the absence of SAW to 0.15 for $\eta=3\times10^{-3}$. The total cw reflection at ω_0, which is given by $r(\omega_0)+2r(\omega_0+\omega_s)$, increases from 0 to 0.50, when the SAW is applied.

The large changes in the reflected intensity induced by the SAW near a Fabry-Perot reflection minimum indicates that the 2D structures can be used as an efficient optical switch in the reflection mode. Since we have exploited the Fabry-Perot oscillation to achieve a vanishing reflection in the absence of SAW, the traditional definition yields a large and undefined value for CR. We plot the total reflection coefficient, instead of CR, as a function of η in Fig. 10. Note that nearly 85% of the light intensity at the frequency ω_0 is reflected for a moderately high, but realistic, dielectric modulation. The reflection through the shifted frequencies changes from 0 (at $\eta=0$) to 0.23 (at $\eta=6\times10^{-3}$).

As indicated in Fig. 1, the SAW wavelength determines the center frequency of the acoustically induced reflection band in the 2D structures. Since the slope of the ω versus $\mathbf{k}$ dispersion is very large, even a small change in $\mathbf{k}_{SAW}$ along with momentun conservation can shift the frequency of the modulated light over a range of 5 THz.[7] In order to calculate the tunability in the present case, we have repeated the calculations by varying λ_{SAW} in the range 5.225–4.95 μm. The corresponding reflection coefficients through the shifted frequency channel are shown in Fig. 11. As expected from the dispersion curve in Fig. 1, the resonant wavelength increases with decreasing SAW wavelength. The increase of the emission bandwidth while maintaining a high acoustic power poses a challenge for the design of the IDTs. In an IDT with fixed finger period, the acoustic power increases with the IDT length, while the band width is inversely proportional to it.[30] The band width can be increased by using tapered IDTs, where the finger separation varies along the IDT length. Another possibility is to use focusing IDT. Here, the IDT length can be reduced while maintaining the acoustic power by increasing the aperture angle.[31] Using either tapered IDT or the focusing IDT, it is possible to obtain a wide band SAW. Notice that a 10% change in SAW wavelength around 5.5 μm can tune the center wavelength of the reflection band over a range of about 4.2 nm, which corresponds to

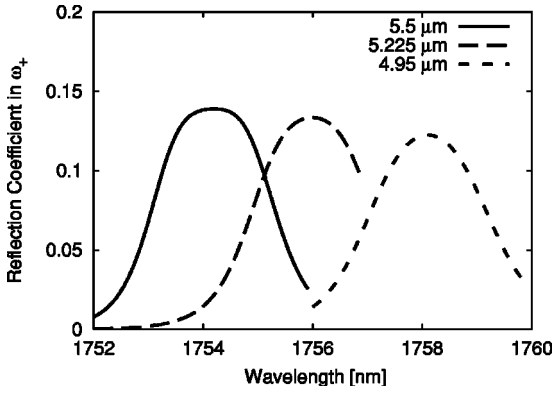

FIG. 11. Reflection coefficient for the up-shifted mode ω_+ of the structure of Fig. 8, calculated for three different SAW wavelengths.

400 GHz. The structure can thus be used as an active filter, which selectively transmits only a narrow band of frequencies. A reliable frequency tunability within the bandwidth requires a very small bandwidth for the reflection spectrum. In the present case, the full width at half maximum is about 150 GHz (cf. Fig. 11). If the studies are carried out using smaller SAW wavelengths on longer PBG structures, we expect much narrower bandwidths and much wider tuning ranges.

The high contrast ratio at ω_0, high reflection coefficients at the shifted frequencies, as well as the tunability of ω_0 a 400 GHz range make the 2D PBG structure modulated by a SAW a serious candidate for optical switches, modulators, and dynamic frequency shifters for DWDM applications. We expect to improve the performance of the devices by reducing the SAW wavelength, increasing the interaction length and acoustic energy density, and optimizing the dimensions of the holes and the lattice parameters.

V. CONCLUSION

We have extended the TM method to study light propagation in PBG structures modulated by acoustic waves and applied this method to obtain the change in the transmission and reflection spectra induced by SAWs in PBG crystals. We show that a large modulation of the light intensity with contrast ratios up to 300 can be obtained in 1D devices based on a cavity resonator. Since the 1D structure employs cavity states with a narrow spectral range to enhance the modulation performance, their frequency tunability becomes very limited.

Two-dimensional structures offer plenty of flexibility for the choice of design parameters such as the device length, the SAW power density and wavelength, the radius of holes, the lattice structure, and the lattice constant. In particular, we have exploited the Fabry-Perot oscillation arising from the finite size of the PBG structure to design fast (switching times less than a 1 μs) photonic switches with a high contrast ratios between the ON and OFF states. A major advantage of the proposed 2D planar device relies on its wavelength tunability within a large bandwidth, which can be achieved by changing the SAW wavelength or the angle of incidence of the incoming light.

ACKNOWLEDGMENTS

The original TM code, written by A. J. Ward and J. B. Pendry, is from the Computer Physics Communication International Program Library. We thank Professor J. B. Pendry for providing additional material to understand their computer code, Dr. A. Reynolds for a discussion on numerical stability. We also thank H. T. Grahn for a careful reading of the manuscript. Financial support (for S.K.) from the Alexander von Humboldt Foundation, Germany, and from the Deutsche Forschungsgemeinschaft (for P.V.S., Project No. 5A598/3-1) is gratefully acknowledged.

[1]For example, Jean-Pierre Laude, *DWDM Fundamentals, Components, and Applications* (Artech House, Norwood, 2002).
[2]J. D. Joannopoulos, R. D. Meade, and J. N. Winn, *Photonic Crystals* (Princeton, 1995).
[3]W. F. Liu, P. St. J. Russell, and L. Dong, Opt. Lett. **22**, 1515 (1997).
[4]K. Busch and S. John, Phys. Rev. Lett. **83**, 967 (1999).
[5]K. Yashino, Y. Shimoda, Y. Kawagishi, K. Nakayama, and M. Ozaki, Appl. Phys. Lett. **75**, 932 (1999).
[6]S. W. Leonard *et al.*, Phys. Rev. B **61**, R2389 (2000).
[7]P. Santos, J. Appl. Phys. **89**, 5060 (2001).
[8]S. Sanchez, C. De Matos, and M. Pugnet, Appl. Phys. Lett. **78**, 3779 (2001).
[9]P. Halevi and F. Ramos-Mendieta, Phys. Rev. Lett. **85**, 1875 (2000).
[10]D. Kang, J. E. Maclennan, N. A. Clark, A. A. Zahidov, and R. H. Baughman, Phys. Rev. Lett. **86**, 4052 (2001).
[11]P. St. J. Russell, Phys. Rev. Lett. **56**, 596 (1986).
[12]P. St. J. Russell, J. Appl. Phys. **59**, 3344 (1986).
[13]P. Hess, Phys. Today **55(3)**, 42 (2002).
[14]C. W. Ruppel *et al.*, IEEE Trans. Ultrason. Ferroelectr. Freq. Control **40**, 438 (1993).
[15]See, for example, N. Goto, Y. Miyazaki, Jpn. J. Appl. Phys., Part 1 **37**, 2947 (1998); and references cited therein.
[16]F. C. Jain and K. K. Bhattacharjee, IEEE Photonics Technol. Lett. **1**, 307 (1989).
[17]C.-K. Sun, J.-C. Liang, and X.-Y. Yu, Phys. Rev. Lett. **84**, 179 (2000).
[18]S Krishnamurthy and P. V. Santos, Appl. Phys. Lett. **83**, 1095 (2003).
[19]J. B. Pendry, J. Mod. Opt. **41**, 209 (1994).
[20]J. B. Pendry, J. Phys.: Condens. Matter **8**, 1085 (1996).
[21]A. J. Ward and J. B. Pendry, J. Mod. Opt. **43**, 773 (1996).
[22]C. T. Chan, Q. L. Yu, and K. M. Ho, Phys. Rev. B **51**, 16635 (1995).
[23]A standing wave made by two IDTs facing each other, each powered with $I/2$, will have an amplitude $(2I)^{1/2}$. The optical modulation, which is proportional to the square of this amplitude is, therefore, more efficient for a standing wave.
[24]M. M. de Lima, P. V. Santos, and R. Hey, Appl. Phys. Lett. **83**, 2997 (2003).
[25]M. M. de Lima, P. V. Santos, R. Hey, and S. Krishnamurthy, Physica E (Amsterdam) **21**, 809 (2004).
[26]D. Labilloy *et al.*, Phys. Rev. Lett. **29**, 4147 (1997).
[27]P. R. Villeneuve, S. Fan, and J. D. Joannaopoulos, Phys. Rev. B **54**, 7837 (1996).
[28]M. Trigo, A. Bruchhausen, A. Fainstein, B. Jusserand, andV. Thiery-Mieg, Phys. Rev. Lett. **89**, 227402 (2002).
[29]S. Y. Chou, P. R. Krauss, and P. J. Renstrom, Appl. Phys. Lett. **67**, 3114 (1995).
[30]M. Streibl, A. Wixforth, J. P. Kotthaus, A. O. Govorov, C. Kadow, and A. C. Gossard, Appl. Phys. Lett. **75**, 4139 (1999).
[31]M. M. de Lima Jr., F. Alsina, W. Seidel, and P. V. Santos, J. Appl. Phys. **94**, 7848 (2003).